

Tribological and Corrosion Behaviors of Titanium Carbonitride Coatings in Simulated Biological Fluid

W. Aperador^{1,*}, A. Delgado¹, E. Vera²

¹ School of Engineering, Universidad Militar Nueva Granada, Bogotá-Colombia

² Universidad Pedagógica y Tecnológica de Colombia, Avenida Central Norte, Km 2, Tunja, Colombia

*E-mail: g.ing.materiales@gmail.com

Received: 18 March 2015 / *Accepted:* 15 April 2015 / *Published:* 28 April 2015

This article contributes to the study of the behavior of the hard coating titanium carbonitride (TiCN) obtained by the technique physical vapor deposition (PVD), using as substrate Bio-medical grade stainless steel 316LVM. The evaluation was conducted using a tribometer, subsequently the electrochemical properties were evaluated by techniques of electrochemical impedance spectroscopy and polarization curves, Finally, a test is made tribocorrosion, by combining these two trials and in a simulated biological fluid. Techniques of scanning electron microscopy and XRD were used to characterize the coatings. TiCN coatings, showed improved performance against corrosion phenomena and abrasive wear than steel 316LVM.

Keywords: titanium carbonitride, wear, corrosion, biomaterial.

1. INTRODUCTION

In surgical implants, corrosion can be a critical phenomenon, which affects both the biocompatibility of the implant as the structural integrity of the prosthesis [1][2]. The corrosion and dissolution of the surface layers of the material are two mechanisms that can lead to the introduction of metal ions in the human body, causing adverse effects on biological reaction thereof [3] [4]. The tribocorrosion is associated with the degradation of the materials when the effect of wear and corrosion are combined simultaneously [5] [6]. Biomaterials do tests required in combination because the implants are subjected to contact with biological fluid and moving charge. To evaluate the performance of these materials, the purpose of this proof is required is carried the synergy between abrasive wear and corrosion [7].

Surgical implants surface treated with deposition of ceramic films have shown excellent resistance to demonstrate phenomena bio corrosion and proves biocompatible, as with TiAlN coatings on stainless steel AISI 316 L, for orthopedic applications. TiAlN films have excellent tribological properties, are resistant to corrosion and also are biocompatible nature, toxicological evaluations of such coatings is confirmed [8]. Research on friction and wear mechanisms -PVD TiAlN coatings on carbon steels, demonstrate that the use of these films greatly reduces friction coefficients and the rate of wear [9].

One of the many properties that are looking for in a biomaterial that is inert in the workplace, however, is unusual case [10]. The human body, as it is an aqueous medium, promoting development of corrosive phenomena on metallic implants, called electrochemical processes. Biocorrosion, has been one of the problems to the durability of implants in the human body faces. Body fluids are highly hostile to the metal, thus, the use of metal alloys, such as bio-implants is limited by the aggressive physiological media [11] [2].

Therefore, the purpose is the fabrication of coatings (TiCN) to provide a combination of successful clinical and economic benefits. To make this possible, it is essential characterization and electrochemical and tribological evaluation of alloys using coatings, biocompatible nature, capable of protecting conventional materials, such as stainless steels

2. EXPERIMENTAL DETAILS

The TiCN films have been grown on Bio-medical grade stainless steel 316LVM substrates (Table 1) by using a multitarget magnetron reactive sputtering technique, with ar.f. source (13.56 MHz) and stoichiometric TiC and Ti targets with 99.9% purity. The deposition parameters for obtaining high-quality coatings were sputtering power of 200 W for TiC and 250 W for the Ti target; substrate temperature 250 °C; under circular rotation substrate with 60 RPM, to facilitate the formation of the stoichiometric film. The sputtering gas was a mixture of Ar 76% and N₂ 24% with a total working pressure of 5.8×10^{-5} mbar, under argon and nitrogen gas flow of 50 sccm and 16 sccm, respectively with a total thickness around 950 nm for all coatings. All substrate surfaces were cleaned of organic contaminants in an ultrasonic bath in the sequence of ethanol and acetone for 15 minutes each. Prior to deposition, the vacuum chamber was evacuated using a turbomolecular pump until a base pressure of 7.2×10^{-5} mbar is attained in order to reduce the effects of residual air. Inside the chamber the substrates were subjected to a bias voltage of -400 V (r.f.) with a potential of 60 W (r.f.) in argon plasma (Ar) for 15 minutes in order to remove other contaminating impurities from the surfaces [2].

Table 1. Chemical composition of steel ASTM F-138, used as substrate.

Fe	Cr	Ni	Mo	Mn	Si	Cu	N	C	S	P
balance	18.8	14.6	3.5	2.2	0.99	0.46	0.12	0.03	0.01	0.025

In order to study the influence of the synergy between abrasive wear and corrosion. Were carried out tests pin-on-disk, according to the standard ASTM G99-05 in an Tribometer NANOVEA MT60 at 37 ° C, in order to evaluate and compare the wear resistance of the coatings study. The wear was measured using a profilometer, Ambios Technology, XP-2 high performance. Tribocorrosion test using equipment Tribometer NANOVEA MT60 was used at a temperature of 37 ± 0.2 ° C (normal body temperature). The test parameters are shown in Table 2. tribometer was adequate with an electrochemical cell consisting of a series of three electrodes, as is the reference (Ag / AgCl), the counter electrode (platinum wire) and work based on a specimen with an area of exposure of the sample of 1 cm². Gamry potentiostat model PCI-4 using the techniques of Electrochemical impedance Spectroscopy and polarization curves - for the evaluation of resistance to corrosion and wear (Figure 1). The polarization curves were measured with a scanning rate of 1 mV / s, in a range of voltages from -250 mV to +250 mV with respect to the corrosion potential (E_{corr}). Nyquist plots were obtained with frequency sweeps between 0.001 Hz and 300 kHz using an amplitude of the sinusoidal signal of 10 mV. The values of corrosion rate (V_{corr}) were calculated from the Tafel slopes and the value of corrosion current density (I_{corr}) in the range of ± 250 mV potential vs. E_{corr}, from anodic polarization curves.

Table 2. Test Parameters

Sliding pattern	alumina balls
Diameter of ball	6 mm
Normal load	5 N
total sliding length	80 m
Velocity	4.7 cm/s

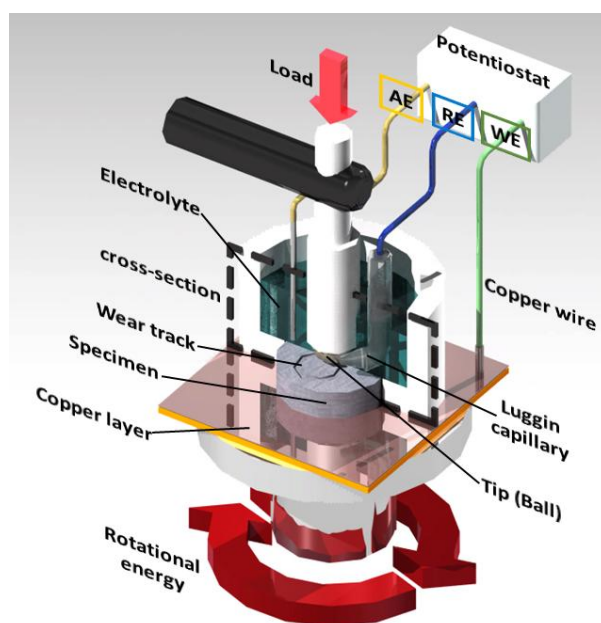


Figure 1. Schematic tribometer adequate equipment for corrosion wear tests

3. RESULTS AND DISCUSSION

3.1 Coating characterization

Fig 2, is shown the coating surface characterization TiCN, is observed in the sample that is a dense structure, compact, in addition a smooth surface, with porosity of varying size and even some tracks left by the sanding process in the substrate, is not observed, detachment of the film, indicating good adhesion.

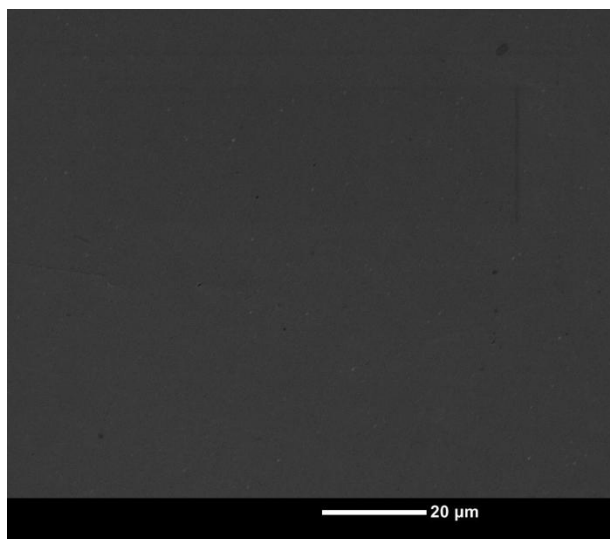


Figure 2. Surface micrograph of the TiCN coatings.

Fig. 3 shows XRD patterns of the substrate, the main diffraction peaks appear at about 43.55° and 50.61° ; 74.65° for a preferential orientation (111) and (220), respectively correspond to signals characteristic of the cubic crystal structure face-centered structure (FCC) and lattice parameter $a = 3.602 \text{ \AA}$ corresponding to Fe in austenitic phase, analysis by the Rietveld method shows 100% of this phase by XRD the plastic deformation of the substrate surface was determined, this was performed by measuring the width of the diffraction peaks at half their height, dislocation density introduced in the material obtaining by polishing a very small value generated plastic deformation corresponding to 0.00032, indicating that the polishing induces a significant increase in strain [12-13].

Fig. 4, the XRD patterns of the TiCN film is observed, who has a crystal cubic face-centered structure (FCC) NaCl type, similar to the structures, TiN (titanium nitride) and TiC (titanium carbide), this type of structure, generates adequate adhesion between the substrate and the coating [14]. However, there seems to be some confusion in the literature about the site occupancy of the different atomic species in the structure of TiCN [15]. The high intensity peaks correspond to the orientation of the Bragg planes (200) and (111) indicating a slightly textured growth along these lines another peak with less intensity corresponding to diffraction flats (220). The presence of Ti CN in the direction, Bragg plane (111) is associated with a substitution mechanism where the C atoms replaced by N atoms resulting in a Ti-organized system and CN disordered, within the NaCl type structure FCC. This result indicates that the gas flow nitrogen directly influences the structure of the coatings of Ti-CN. When the

flow of nitrogen gas is about 16 sccm and the rf bias voltage it is -60V, facilitating access of N, the FCC structure, thus resulting in a partially ordered structure of Ti atoms and vacancies in nonmetallic sublattice [16].

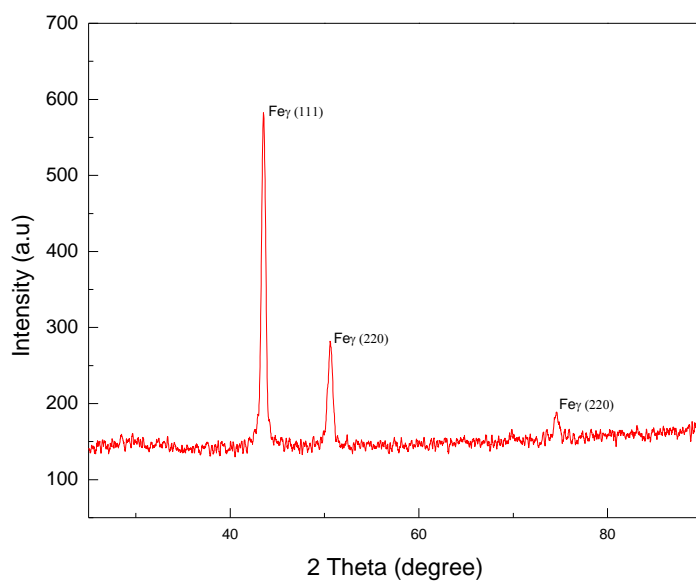


Figure 3. XRD substrate where shown the characteristic patterns, the austenitic steel, after mechanical preparation.

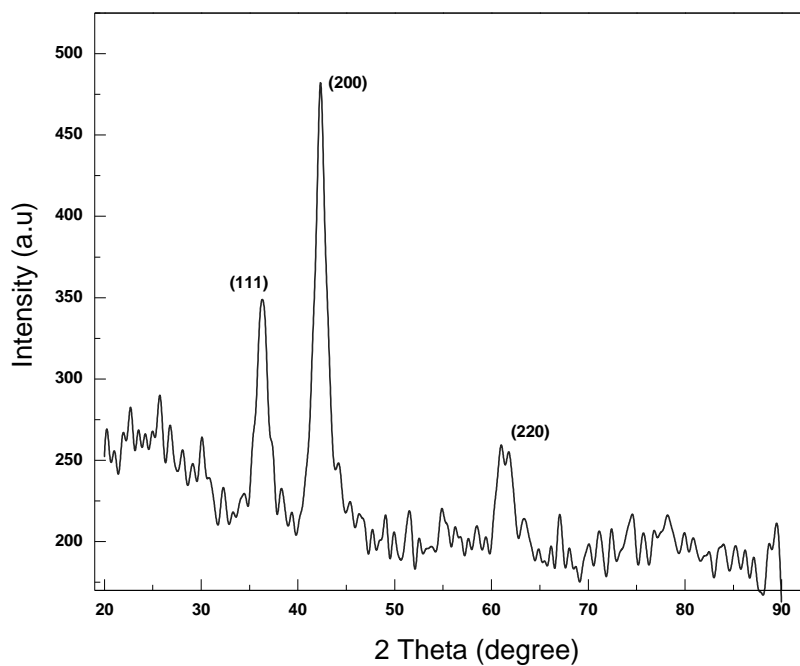


Figure 4. XRD diffraction patterns TiCN where they meet the crystalline planes associated to substitution mechanisms.

3.2 Electrochemical measurements because there are two methods – EIS and potentiodynamic polarization.

In Figure 5 are shown Nyquist plots for the coating of titanium carbonitride, measurements were made at immersion times of 1, 7, 14 and 28 days. The evaluation was carried out during this time due to a stabilization of the total impedance, after 28 days was observed. The impedance module at low frequencies exhibits similar behavior in each of the tests performed, therefore it can be considered that the rate of corrosion resistance and are similar, the difference is determined at intermediate frequencies as they are obtained, different values of total impedance this is due to the reactions which are generated on the surface the coating in each of the times studied [16]. With regard to the constant phase element is that the behavior of the coating is having an increased depending on the time of an accelerated manner for the first 7 days, at 14 days these values are stable, after 21 days this value has similar values to that found previously indicating that its response is of nature capacitive. The coatings show for the first 7 days of immersion in impedance spectra two intensity peaks in the phase angle, this is due to the electrolyte enter for the pores reaching the substrate to form a passive oxide film, however, as recorded, in the Nyquist plots, of these films to 21 days immersion suggested that the pores of said multilayers, stoppered with the oxide generated.

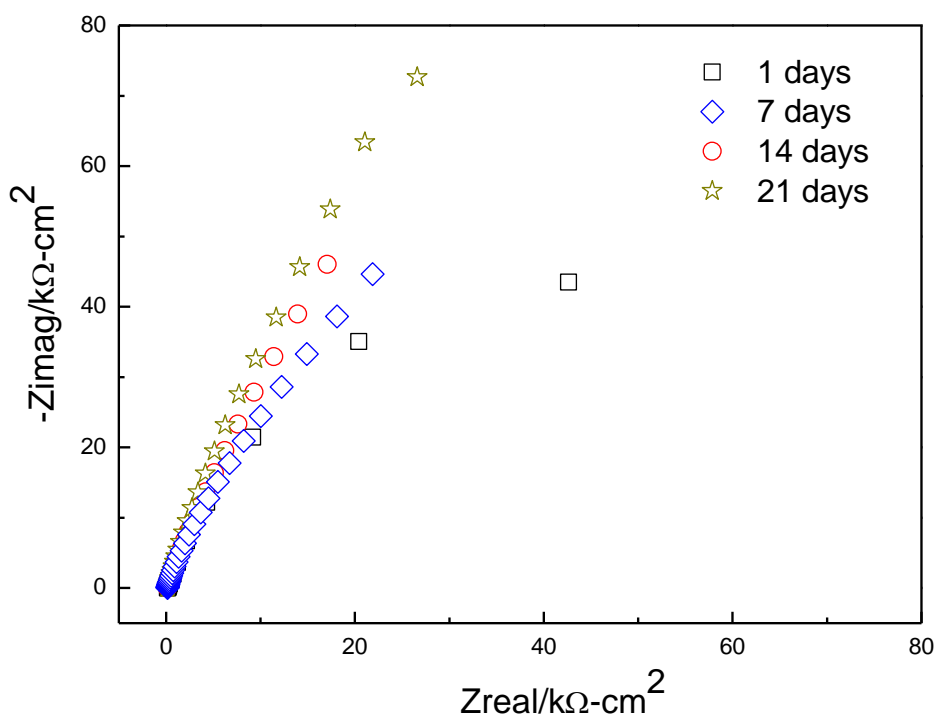


Figure 5. Nyquist diagrams corresponding to the tests carried out at TiCN coating deposited on steel 316LVM, after evaluation in the solution, simulated at different times.

The circuit of Figure 6 shows a first resistance (R_r + s) associated with the simulated solution ringers lactate known, this is found at high frequencies 300 kHz; then there is a CP1 and resistor associated to the first elements, which are detected in the coating, these elements may be due to any

feedback or surface absorption of some of the species with the entry of simulated fluid then intermediate frequencies is possible to find other elements such as a CPE2 and a resistor, these elements are associated at the interfacial transition zone between the coating and the adhesive layer and titanium nitride which form the coating, domain low frequency is normally found the process of charge transfer in combination with the process of mass transfer this corresponds to the last R2 and CPE2 these elements are located in the corresponding interfacial area the interfacial coating zone and steel biocompatible [17].

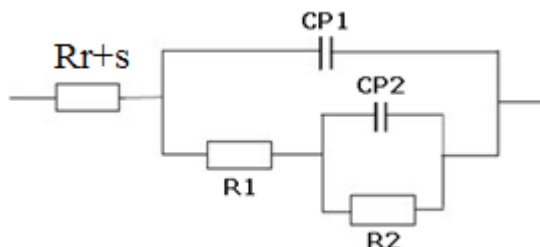


Figure 6. Electrical circuit used to simulate the electrochemical characterization of coatings in contact with the simulated fluid.

Fig 7, the polarization curves of the coated steel and exposed to the fluid are observed, The first analysis is performed with respect to the corrosion potential where it is obtained which as it progresses, the time of evaluation, is obtained, the potential of corrosion of these is more positive and therefore there is a lower tendency to corrode in the midst of simulated solution, the difference of potential indicates that has been generated a mechanism of protection due to the protective layer that stabilizes. With respect to the corrosion current density can be established which is influenced with regard to the evaluation time due to that extent that the evaluation time increases generate lower density values corrosion, suggesting a structure homogeneous and stable since it does not dissolve.

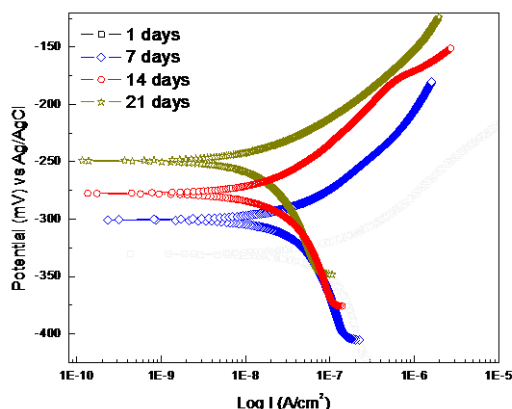


Figure 7. Tafel polarization curves, after evaluating the TiCN coating, a function of time up to 21 days.

3.3 Tribocorrosion

In Figure 8, attrition rates are observed, assembly made to make this type of test is shown in Figure 1, where can be evaluated the mechanical wear generated by contact of the sphere alumina and then the steel on the coating, additionally was placed in contact with the fluid simulated [18]. The assay can determine the coefficient of friction. Regarding coefficient of friction steel AISI 316LVM uncoated generates a high value in the coefficient of friction (μ) at initial contact reaching a value of $\mu = 0.55$, subsequently were performed this same type of test coatings obtaining low friction values. This is due to the hardness of the interstitial carbonitrides, which are in the crystalline structure of these coatings. Measured friction coefficients, show a progressive decrease by increasing, the evaluation time and this is due to that, there is an effect of generation of passive layer, which generates it; an additional hardness to the system, this protective layer is stabilized, depending on the proximity to the 21-day evaluation period.

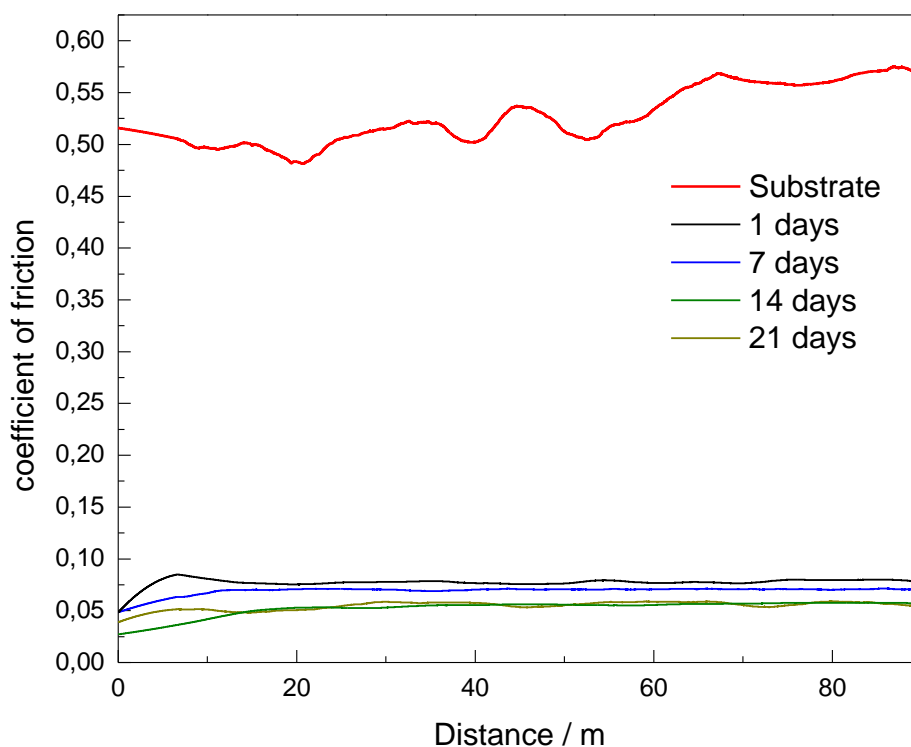


Figure 8. Wear curved substrate and the coating; immersed in a solution containing ringers lactate.

4. CONCLUSIONS

TiCN coatings were deposited by reactive r.f. magnetron sputtering by using simultaneous deposition from TiC and Ti targets in N_2+Ar mixture. Using the techniques of scanning electron microscopy and X-ray diffraction, the coated surfaces are characterized, determining a adequate

adhesion. With respect to electrochemical characterization techniques, it was determined that when the evaluation time increases, the voltage decreases corrosion, towards more noble values, indicating protection; featuring coatings; Corrosion caused by simulated solution. Regarding wear curves may be determine the coefficients of friction are minimal compared to the substrate this value is decreasing as evaluated over time this value is stable after 21 days testing.

ACKNOWLEDGEMENTS

Thanks the financial support from the Universidad Militar Nueva Granada, contract number ING-1775-2015.

References

1. Y. Y Guu, J. F. Lin, C. F. Ai, *Thin Solid Films*, 287 (1996) 16
2. W. Aperador, J. Duque, E. Ruiz, *Adv Mat Res*, 1016 (2014) 320
3. Y. Y Guu, J F Lin, *Surf. Coat. Technol*, 85 (1996) 146
4. C. Wei, J. F. Lin, T-H Jiang, C-F Ai, *Thin Solid Films*, 381 (2001) 104
5. P.K. Ajikumar, M. Kamruddin, S. Kalavathi, A.K. Balamurugan, S. Kataria, P. Shankar, A.K. Tyagi, Synthesis, *Ceram. Int*, 38 (2012) 2253
6. J. Zhang, Q. Xue, S. Li, *Appl. Surf. Sci.*, 280 (2013) 626
7. P.K. Ajikumar, M. Kamruddin, T.R. Ravindran, S. Kalavathi, A.K. Tyagi, *Ceram. Int*, 40 (2014) 10523
8. S. Hogmark, S. Jacobson, M. Larsson, *Wear*, 246 (2000) 20
9. D.G. Bansal, O.L. Eryilmaz, P.J. Blau, *Wear*, 271 (2011) 2006
10. A Forn, J.A Picas, G.G Fuentes, E Elizalde, Mechanical and tribological properties of TiC_xN_{1-x} wear resistant coatings, *Int. J. Refract. Met. Hard Mater*, 19 (2001) 507
11. D. Munteanu, C. Gabor, D.G. Constantin, B. Varga, R. Adochite, O.C. Andrei, J.M. Chappé, L. Cunha, C. Moura, F. Vaz, *Tribol. Int*, 44 (2011) 820
12. S. Hassani, J.-E. Klemberg-Sapieha, L. Martinu, *Surf. Coat. Technol*, 205 (2010), 1426
13. F. Cai, X. Huang, Q. Yang, *Wear*, 324–325 (2015) 27
14. V. S. Calderon, J.C. Sánchez-López, A. Cavaleiro, S. Carvalho, *J. Mech. Behav. Biomed. Mater*, 41 (2015) 83
15. X. Zhang, Y. Qiu, Z. Tan, J. Lin, A. Xu, Y. Zeng, J.J. Moore, J. Jiang, *J. Alloys Compd*, 617 (2014) 81
16. A.M. Abd El-Rahman, Ronghua Wei, *Surf. Coat. Technol*, 258 (2014) 320
17. J.C. Caicedo, C. Amaya, G. Cabrera, J. Esteve, W. Aperador, M.E. Gómez, P. Prieto, *Thin Solid Films*, 519 (2011) 6362
18. T. Borkar, S. Nag, Y. Ren, J. Tiley, R. Banerjee, *J. Alloys Compd.*, 617 (2014) 933
19. S. Buchholz, Z.N. Farhat, G.J. Kipouros, K.P. Plucknett, *Int. J. Refract. Met. Hard Mater*, 33 (2012) 44